Available at: http://www.ictp.it/~pub_off IC/2004/96

United Nations Educational Scientific and Cultural Organization
and
International Atomic Energy Agency

THE ABDUS SALAM INTERNATIONAL CENTRE FOR THEORETICAL PHYSICS

# A NEW APPROACH TO ELECTRICAL IMPEDANCE IMAGING TECHNIQUE

Kamila Afroj Quadir[1],
*Biomedical Physics Group, Department of Physics, University of Dhaka, Dhaka, Bangladesh*
*and*
*The Abdus Salam International Centre for Theoretical Physics, Trieste, Italy,*

Fuad Nasir[2], Mahmudur Rahman and K.S. Rabbani
*Biomedical Physics Group, Department of Physics, University of Dhaka, Dhaka, Bangladesh*.

**Abstract**

It is possible to obtain a 2 dimensional (2D) image of a volume conductor, to locate a few widely separated objects, by driving ac constant currents through two orthogonal pairs of electrodes and measuring the resulting potential differences between several diagonally placed electrodes at the centre and back-projecting their impedance values along equi-potential lines. This has been termed as Pigeon Hole Imaging (PHI). Experimental verification has been attempted using a small insulating object placed at different locations in a saline filled 2D phantom. For a 6 x 6 matrix, the image in 16 pixels in close proximity of the diagonal along which electrodes are arranged, coincide with the object positions, while they do not for the remaining 20 pixels. We applied a new technique where image smearing patterns have been used to correct the images in 14 of these pixels while 6 pixels near the two opposite corners still remain uncertain. Thus 30 pixels out of 36 give the right object position which may be termed a success. The concept may be extended further to higher order matrices by increasing the number of diagonal electrodes. The present work mainly concentrates on the feasibility of localization of a single small object in one matrix position of the image.

MIRAMARE – TRIESTE

September 2004

[1] Regular Associate of ICTP. kamila@dhaka.com
[2] Student intern at Dhaka University from Centre College, USA.

# INTRODUCTION

Conventional Four-Electrode Impedance Measurement (FEIM) is a simple technique where current is driven between a pair of electrodes and potential difference is measured between another pair to avoid the effects of contact resistance [1]. In a volume conductor the zone of sensitivity of this measurement is rather wide and it is difficult to study a small region isolated from its surroundings. When applied on a human body to study a specific organ, the measured value includes the effects of other organs in the vicinity which make the interpretations difficult and unreliable [2]. A significant development in impedance measurements was the introduction of Electrical Impedance Tomography (EIT) which provides images of tissue impedance distribution [3,4,5]. Although the resolution offered by EIT is poor compared with other imaging modalities (about 10% for a 16-electrode system), for studies of large organs like heart, lungs and stomach, even such degree of resolution is often not required. Therefore, it appears that technologies bridging the intermediate region may have useful applications. With this in mind, a new method named as Focused Impedance Measurement (FIM) was developed earlier in the Biomedical Physics Laboratory of University of Dhaka [6,7], which essentially is a combination of two FEIM systems placed orthogonally, centred around the zone of interest. The sum of the impedances from these two orthogonal measurements result in a greater contribution from the central zone of interest, thus contributing to a focusing effect. In a further development, by placing two potential measuring electrodes diagonally in the central region, the requirement of the number of electrodes was reduced from 8 to 6. The method was successful in experimental measurements on phantoms and on the human body for gastric emptying studies.

By increasing the number of diagonally placed electrodes in the above mentioned FIM and employing a simple method of backprojection, a new imaging modality was developed at the Biomedical Physics Laboratory of Dhaka University which was termed as Pigeon Hole Imaging (PHI). This is briefly described below for a 6x6 matrix which employs seven diagonal electrodes. For a 6 x 6 matrix, the image in 16 pixels, in close proximity of the diagonal along which electrodes are arranged, coincide with the object positions. An innovative new technique where image smearing patterns have been used to correct the images in 14 pixels while 6 pixels near the two opposite corners still remain uncertain. Thus 30 pixels out of 36 give the right object position which may be termed a success. The concept may be extended further to higher order matrices by increasing the number of diagonal electrodes. The present work mainly concentrates on the feasibility of localization of a single small object in one matrix position of the image.

## MATERIALS & METHODS

### *A. Concept of PHI*

For conceptual clarity, the method is being explained with a 2X2 matrix example. However, the process is scalable, simply by increasing the number of diagonally placed electrodes within the same region, the number of pixels can be increased, such as 3 x 3 matrix, 4 x 4 matrix, and so on.

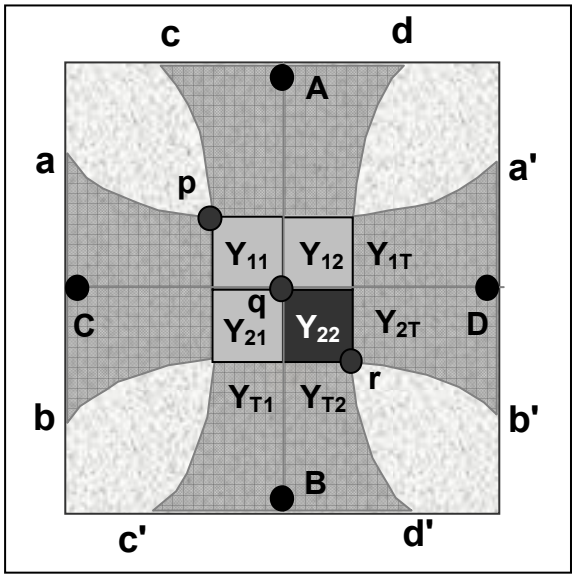


Fig.1. Basis of Pigeon Hole Imaging

The whole of the shaded square in Fig. 1 represents a segment of a volume conductor seen from outside a surface. An alternating current of constant amplitude is driven once through the pair of electrodes AB, and once through CD, the potential measuring electrodes being p, q and r respectively. The equipotentials through these electrodes when current is driven through the pair AB are shown as aa', CD, and bb'. Similarly those for current-drive pair CD are cc', AB, and dd'. Since the currents are constant in both the directions, for current driven through AB, the inverse of potential measured between p & q gives the total admittance $Y_{1T}$ of the zone bounded by the equipotentials aa' and CD. Similarly, that between q & r gives $Y_{2T}$ of the zone bounded by the equipotentials CD and bb'. Again, for current driven through CD, the inverse of potential measured between p and q gives the total admittance $Y_{T1}$ of the zone bounded by the equipotentials cc' and AB, and that between q & r gives total admittance $Y_{T2}$ between AB and dd'. In all cases, the sensitivity decreases away from the centre.

We assume that the contribution of the zones outside the four central squares are negligible and that these squares have isotropic admittances, $Y_{11}$, $Y_{12}$, $Y_{21}$ and $Y_{22}$ respectively as shown in figure 1. Therefore,

$$Y_{1T} = Y_{11} + Y_{12}\,, \qquad Y_{2T} = Y_{21} + Y_{22}\,,$$
$$Y_{T1} = Y_{11} + Y_{21}\,, \qquad Y_{T2} = Y_{12} + Y_{22}\,.$$

In a measurement, only the four totals are known, and it is required to obtain the admittance distribution in the four pixels from these measured data values.

To obtain a relative admittance distribution, we simply backproject the measured total admittances along the two orthogonal directions. Thus the backprojected values (with a superscript B) are,

$$
\begin{aligned}
Y^B_{11} &= Y_{1T} + Y_{T1} = 2Y_{11} + Y_{12} + Y_{21} \\
Y^B_{12} &= Y_{1T} + Y_{T2} = 2Y_{12} + Y_{11} + Y_{22} \\
Y^B_{21} &= Y_{2T} + Y_{T1} = 2Y_{21} + Y_{11} + Y_{22} \\
Y^B_{22} &= Y_{2T} + Y_{T2} = 2Y_{22} + Y_{21} + Y_{12}
\end{aligned}
$$

In the above backprojected values it can be seen that the individual pixel admittance dominates in each thus giving an image of admittance distribution. There is some contribution from two adjacent vertical and horizontal pixels giving the star burst effect, which can be reduced using suitable filtering.

For the difference image, a small object of different admittance was introduced in one of the matrix positions. The change in admittance, $\Delta Y_{22}$, will occur in element $Y_{22}$ but not in others. Therefore:

$$
\begin{aligned}
\Delta Y^B_{11} &= 0 \\
\Delta Y^B_{12} &= \Delta Y_{22} \\
\Delta Y^B_{21} &= \Delta Y_{22} \\
\Delta Y^B_{22} &= 2\Delta Y_{22}
\end{aligned}
$$

Thus the contrast improves in this difference image, however, the star-burst effect still present.

It needs to be mentioned that while we take the measurements between the equipotential lines, we can either measure the impedance or the admittance of the conducting medium. For simplicity of calculation for PHI, we chose the latter.

### *B. Image Smearing*

In the 6x6 matrix of PHI, where a single object was placed at each of the matrix positions. Out of these, 16 positions along the diagonal of electrodes and at it's close proximity gave correct positions in the corresponding images. However, for the other matrix positions the images did not give the exact object positions. However the smearing pattern of these images appeared to be systematic. This can be expected, as the current flow pattern will depend on the geometry of the electrodes and the object placed in a uniform conducting medium. A back-tracking technique, depending on the smearing pattern was applied which resulted in correction of 14 of the remaining 20 matrix positions.

### *C. Experimental arrangement and measurements*

A 2D phantom was employed for the purpose of measuring the sensitivity of PHI. The container was made of plastic wood with inside dimensions 17.5cm x 17.5cm x 5cm as shown in Fig 2. Seven

potential measurement electrodes were fixed diagonally in the central region such that the vertical and horizontal separations were 1.5 cm each. This produced 36 square elements in a 6x6 matrix. AB and CD were used as the current driving electrodes.

Saline was poured to a depth of 1.5 cm in the 2-D phantom. The conductivity of the saline was adjusted (≅4mS) to obtain potential values that gave maximum sensitivity in the digital voltmeters used. An insulated cylinder (made of plastic) with a diameter of 0.6 cm was used to simulate an object with a different impedance value. This was placed within the saline in the phantom at positions corresponding to different elements in the matrix and voltage readings were taken for PHI. Readings were also taken without the cylinder for calculation of the background admittance distribution.

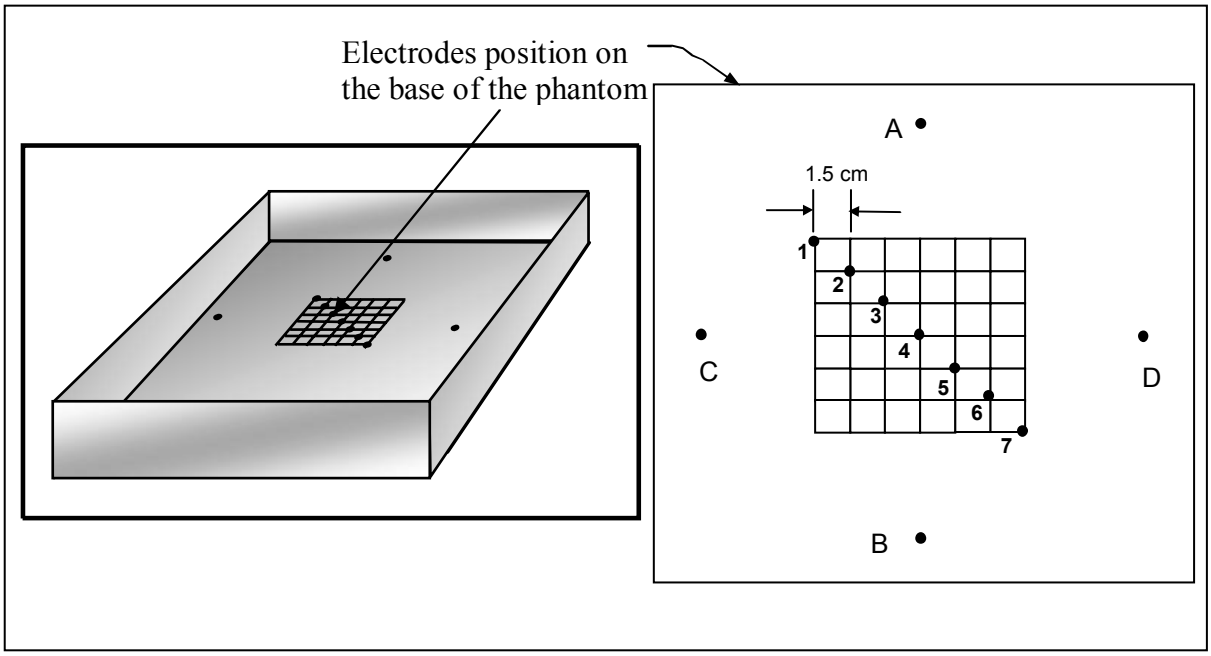


Fig.2. The placements and spacing of electrodes is showing for the 2D phantom

For experiment, we connected one pair of the current drive electrodes (AB in Figure 2) to the constant current driving source and measured the output voltage from the measuring electrodes (between two adjacent pair of electrodes at a time). To reduce errors, we reversed the connections to the measuring electrodes for each configuration and took the average of the measured potentials. After performing all the measurement, we changed to the other current driving electrodes at right angles to the former (CD in Figure 2) and collected data using the same procedure.

The above procedure was repeated by placing an insulated sphere of 0.6 cm diameter (made of plastic) within the saline in the phantom at different matrix elements.

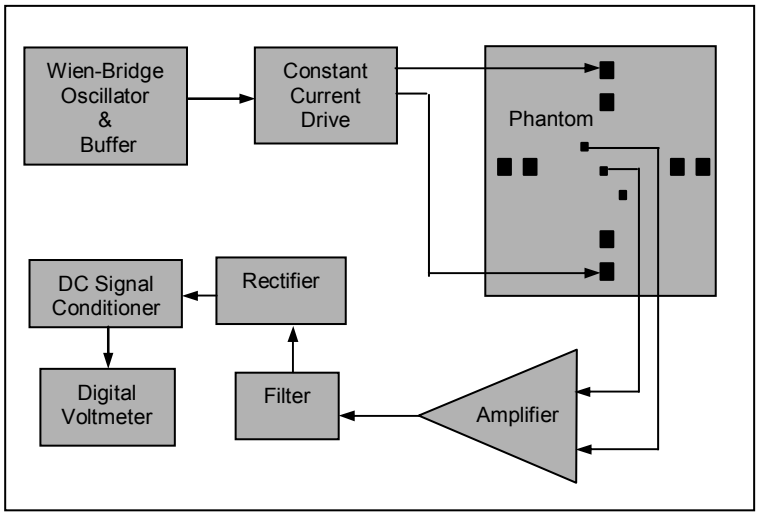


Fig.3. The basic instrumentation of the PHI system

Figure 3 shows the block diagram of the basic instrumentation which was developed and used for manual recordings in order to study the feasibility of the concept. A constant amplitude sinusoidal alternating current of about 30 KHz is fed to a pair of current drive electrodes (outer vertical electrodes shown in Figure 3). The potential developed between an adjacent pair of the three diagonal electrodes is amplified, filtered, rectified and smoothed to obtain a DC voltage, which is measured using a digital voltmeter. Since the current is constant, the inverse of the measured voltage is proportional to the corresponding admittance.

## RESULTS & DISCUSSIONS

Simple backprojected difference images of admittance for the 6 x 6 matrix were reconstructed for all the 36 object positions. It was found that the image positions agreed with the target object locations for 6 pixels on the diagonal along which the potential measuring electrodes were placed (electrode-diagonal) and for 10 adjacent pixels on both sides of this diagonal. These positions are shown in Fig.4 by black shading. For the rest 20 pixels, the image positions changed a little from the target locations. However, a systematic shift towards the electode-diagonal was observed.

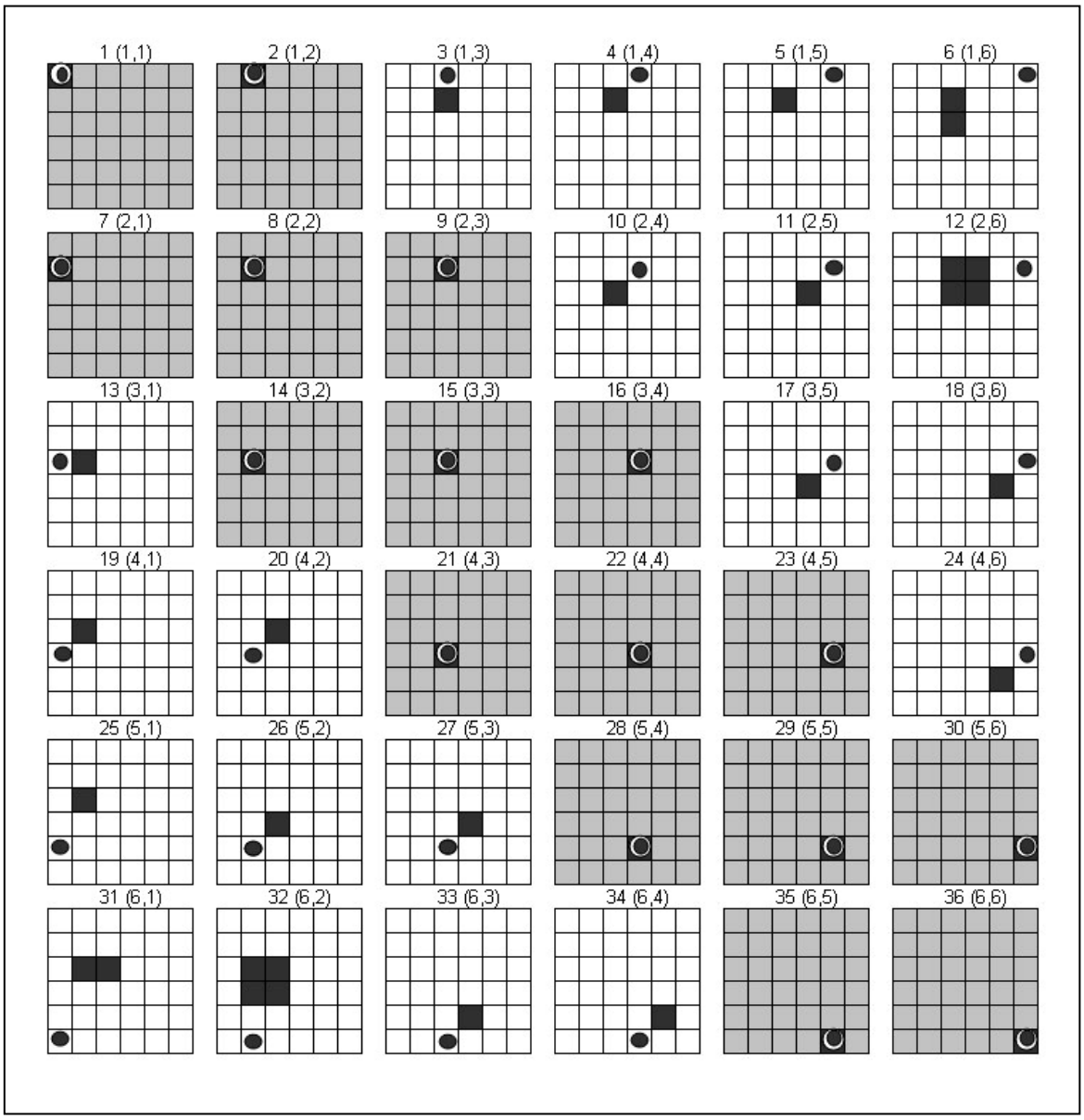


Fig.4. The images for which the target position coincides with the image position are shown shaded

In order to correct the images for the other positions we applied a new method where patterns of image smearing has been used and is described in the next section in detail.

*A. Image Correction Using the New Smearing Technique*

It was observed that where the images missed that actual position, there appeared a systematic shift or spreading of image (or smearing) almost enclosing the target position from both sides. Figure 5 shows the smearing of the images for all the 36 sets. Here only four levels of densities were used to shade the image pixels and only those pixels have been shaded which had pixel values greater than 50% of the maximum in each of the image. This led to an idea that the smearing pattern in the images may be used to correct the image positions. This can be justified, since the current lines and equipotential lines in the phantom will have definite patterns with the object in different pixel positions, therefore the smearing pattern may be unique for each pixel.

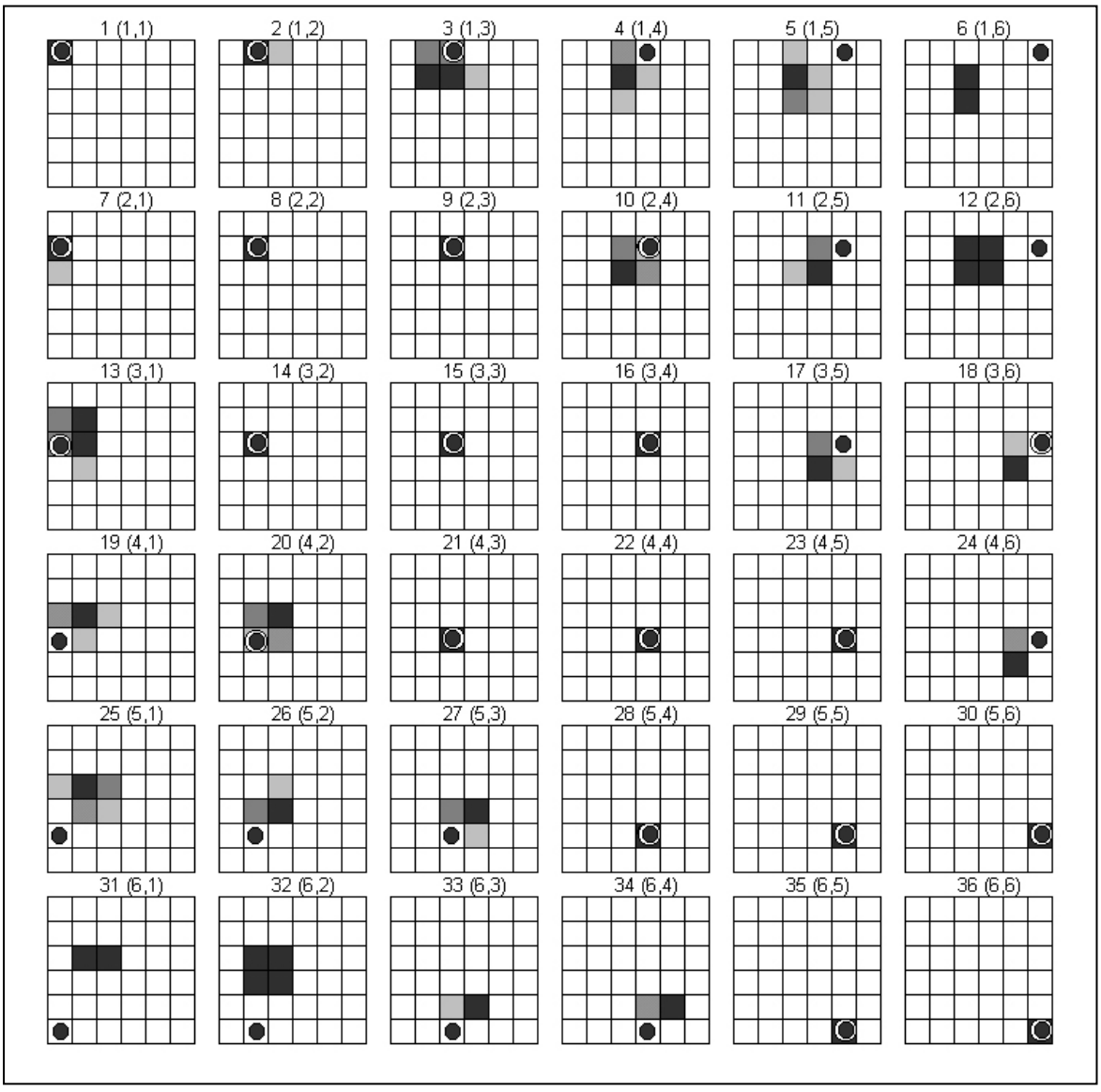


Fig.5. Image smearing down to 50% value of the maximum pixel. value

For convenience of identification, each image in Figure 5 has been given a reference number (1 to 36) together with the matrix element of the target position of the object. We can see that for images 1, 8, 15, 22, 29 and 36 for which the target was placed along the diagonal of electrodes, there is no smearing of images. Similarly images 14, 21, 28 and 35 adjacent to the electrode-diagonal, there is no image smearing while for 7 along the same line parallel to the electrode-diagonal there is slight smearing in one direction only which can be neglected. In all the above image sets the image maximum correspond to the target object position well. Based on symmetry we can also say the same for the image 2, 9, 16, 23 and 30, which are on the other side of the electrode-diagonal.

Now, let us concentrate on Image 20 for target object at position (4,2). The highest pixel value in the image occurs at (3,3), with smearing going to adjacent (3,2) and (4,3) positions. Since we are not supposed to know the target object position beforehand we might be confused whether or not the densest image position at (3,3) represents the target position. If we compare this image with Image 15, which corresponds to the target position of (3,3), we will see that there is no smearing in the latter image. Therefore just the presence of smearing, and that in two directions would give us a hint that in our system the maximum pixel value position is not the target object position. From our knowledge of the target position, (4,2), it appears that the smearing pattern has enclosed its position from both sides as shown in Fig.6a.

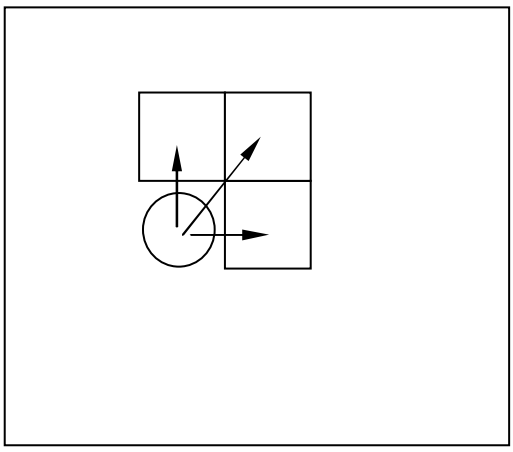

Fig.6a. Spreading or smearing of image from object at position (4,2).

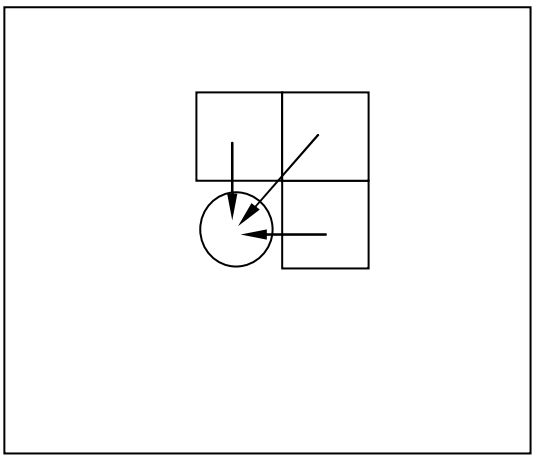

Fig.6b. Tracking back the object position from the smeared pattern.

It appears in Figure 6a that the object has spread out its image northwards, northeastward and eastward. Therefore, such a smear pattern in the image would tell us that the object position is different from the image maximum, and that the target position can be deciphered by back-tracking the expected image shift as shown if Fig 6b.

Images 13, 27 and 34 of Fig 5, which aligns with image 20 along a line parallel to the electrode-diagonal observe a similar pattern of image smearing from which the target position can be obtained, using the same technique as described above. Image 34 has smearing only westwards. Besides image 29, of Fig.5, with image maximum at the same position (5,5) there is no smearing at all and therefore is different from Image 34.

Thus we can correct the target object positions for images 13, 20, 27 and 34 using this 'image smear pattern' technique. Similar patterns of image smear can be observed for images 19, 26 and 33. Of course it can be seen that the pixel values for these images are very small since the target object is far away from the diagonal. Therefore errors in measurements are increased. For images 25, 32 and 31, of Fig.5, the pixel values are very small and it is difficult to make any comments on the image smear pattern. However, some pattern may be identified in images 25 and 31 as shown in Fig. 7a and 7b.

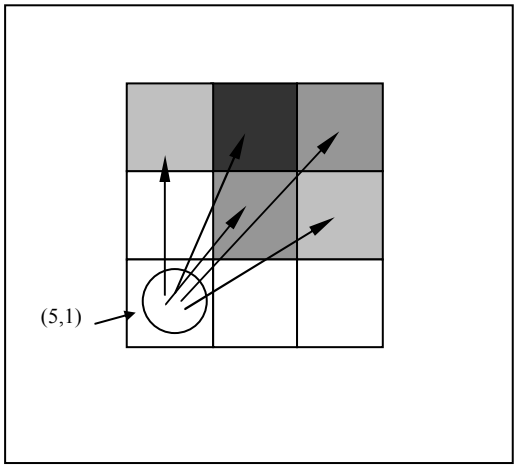


Fig.7a. Image smear pattern of object in position (5,1)

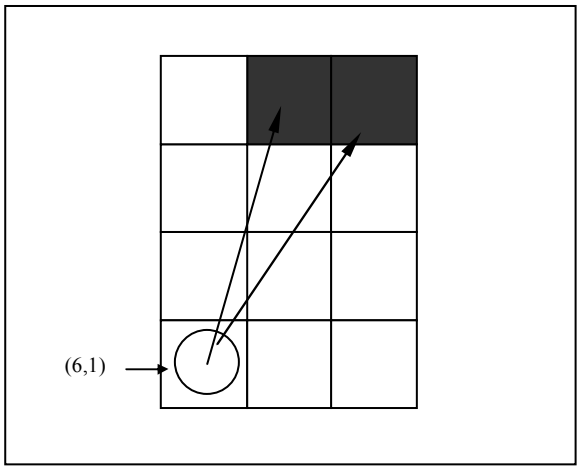


Fig.7b. Image smear pattern for object in position (6,1)

Since these pixel values are too small we are not claiming these patterns to give useful results but are presented to give some indications only. For the target positions on the other side of the electrode-diagonal we get symmetrical results.

The images in Figure 5 can therefore be classified by the following *Image Rules*:

Summarizing the above results we can state the following rules for imaging of a single object using PHI, where images are drawn down to 50% of the maximum pixel value in each image. The rules are stated referred to group identifications of target positions given in the previous section.

1. **16** target positions whose centers are within 0.5 pixel-diagonal of the electrode-diagonal, the image does not smear out and the image maximum corresponds to the target position.

2. **14** target positions whose centers are between 0.5 and 1.5 pixel-diagonal of the electrodes-diagonal, the image smears out asymmetrically in two perpendicular directions from the image maximum. In this case the image maximum does not correspond to the target position, which can be identified by the matrix position that is enclosed or bracketed by the smeared image pattern, whose center is 0.5 pixel-diagonal away from the center of the image maximum.

3. **6** target positions whose centers cannot be ascertained by the present work as it does not show any symmetric pattern, nor was the instrumental sensitivity adequate. The patterns indicated in this work for these two groups will need further work for confirmation.

Thus using the above image rules we can determine the positions of a single object in 30 out of the 36 matrix positions in a PHI system with 7 potential electrodes as shown by the shaded positions in Fig.8, the dark ones indicating where the targets are correctly imaged and the gray ones indicating where the target can be determined using the correction rules presented here based on image smearing.

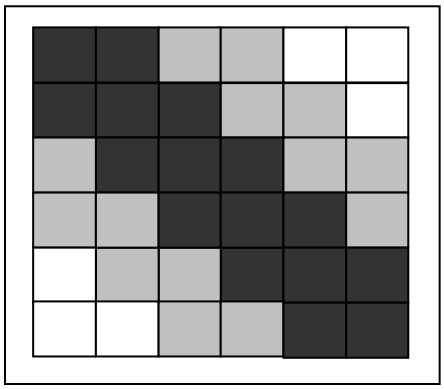

Fig. 8. The total matrix positions for which PHI image localizes a single object

## CONCLUSIONS

The proposed PHI Imaging system has potential for imaging of human body. With the incorporation of correction procedure based on image smearing, it was possible to get the image position correct for 30 of the 36 matrix positions in a 6X6 matrix image.

Although the image is very crude, the technique is versatile because of its simplicity. The spatial resolution can be changed simply by changing the separation of the diagonal electrodes, leaving the current drive electrodes unchanged. Thus depending on the outcome of an initial measurement, the separation of the potential measuring electrodes can be adjusted to locate a non-uniformity with a better resolution.

The measurements for PHI can be easily made using surface electrodes on the human body. In most situations the positions of the target objects (organs) to be imaged are known beforehand and this can be used in judicious placement of electrodes to obtain useful results with the minimum number of trials.

Multi-frequency instrumentation for PHI would be relatively less complex than that for EIT and more importantly, would offer more affordable solutions in the possible diagnosis of tumours that are close to the skin surface. Thus Pigeon-Hole Imaging (PHI) offers a practical imaging modality. In certain applications PHI and FIM can both be used together, PHI being used to locate an organ first, and then FIM to study the time variation of the admittance (or impedance) changes of that organ. Finally both the FIM and PHI techniques may be useful in other areas of science, such as in Geology and Oceanography, where impedance measurements can offer some information about the structure below.

ACKNOWLEDGEMENTS

The authors would like to thank the Department of Physics, University of Dhaka for its kind permission to use the Biomedical Research Laboratories to do the research work.

This work was done within the framework of the Associateship Scheme of the Abdus Salam International Centre for Theoretical Physics, Trieste, Italy. Financial support from the Swedish International Development Cooperation Agency is acknowledged.

REFERENCES

1. Ackmann J J, Sietz M A 1984 Methods of complex impedance measurements in biologic tissue, *CRC crit Rev in Biomed Eng*, 11: 281 – 311.
2. M. Rahman, 1994 Development of a four electrode impedance measurement system for gastric emptying and gastric acid secretion studies. M.Sc. Thesis, University of Dhaka, Bangladesh.
3. D.C. Barber, & B.H. Brown, 1984 Applied Potential Tomography. J. Phys. E: Sci. Instrum, V.17: 723-733.
4. Webster J G 1990 Electrical Impedance Tomography, 1st ed, Adam Hilger, Bristol and New York, 107-131.
5. K.S. Rabbani, M. Hasan, A.B.M.H. Kabir, M. Ahmed & S. Nahar, 1995 Electrical Impedance Tomography (EIT) in the frontal plane using ring electrode configuration. Proceedings, Regional Conference of the IEEE Engineering in Medicine & Biology Society and 14th Annual Conference of the Biomedical Engineering Society of India, New Delhi, India: 1.43-1.44.
6. K.S. Rabbani, M. Sarker, M.H.R. Akond & T. Akter, 1998 Focused Impedance Measurement (FIM) – a new technique with improved zone localisation, Proceedings, X International Conference on Electrical Bio-impedance, Barcelona, Spain: p.31-34.
7. K.S. Rabbani, M. Sarker, M.H.R. Akond & T. Akter, (1999) Focused Impedance Measurement (FIM) – a new technique with improved zone localisation. Annals of the New York Academy of Science, Electrical Bioimpedance Methods, vol.873, p 408-420.